

Using Artificial Neural Networks to Optimize Acceleration Due to Gravity ‘g’ Measurement in a Compound Pendulum Experiment

Sudakhina Prusty¹, Raja Das², and Saralasarita Mohanty^{*1}

¹School of Physical Sciences, National Institute of Science Education and Research, Jatni 752050, India

²Department of Mathematics, School of Advanced Sciences, Vellore Institute of Technology, Vellore, 632 014, Tamil Nadu, India

April 3, 2025

I. Abstract

In this study, we explore a novel approach of implementing the Artificial Neural Network (ANN) model to validate a traditional experiment performed in the undergraduate physics laboratory, e.g. measurement of acceleration due to gravity ‘g’ using compound pendulum. The input layer for the ANN model comprises of different parameters of the compound pendulum experiment such as its effective length, time period of oscillation and initial angular displacement. The model is first trained by using 70 percent of the experimental data. Then the trained model is validated and tested on the rest 30 percent of the experimental data which are treated as unseen data to predict the value of ‘g’. The ANN-predicted values are compared with the experimental value of ‘g’ to assess precision. The average value of ‘g’ was determined to be 1009.029797cm/s^2 with a random error of $\pm 6.817633\text{ cm/s}^2$ through traditional experiment. However, the ANN-predicted value of g was 1009.029858 with a mean absolute error of 0.000592 cm/s^2 . By examining the precision of ANN predictions, the study highlights the advantages and limitations of using machine learning techniques in analyzing physical systems. Additionally, the authors propose that ANN-based methodologies could bridge the gap between theoretical understanding and practical application by introducing students to cutting-edge computational techniques. Such integration allows for a deeper engagement with the subject matter, encouraging critical thinking and problem-solving skills in experimental physics. This innovative approach underscores the transformative role of machine learning in modern physics education. The model’s performance demonstrates high accuracy and robustness in predicting g, outperforming traditional empirical approaches. Our results indicate that ANN-based optimization can significantly improve the precision of gravitational measurements, offering a reliable and efficient tool for applications that require high-accuracy determination of gravitational acceleration.

* Saralasarita Mohanty, saralasarita@niser.ac.in

II. Introduction

The pendulum remains a classic example in physics, demonstrating principles of inertia, gravity, and oscillation[1–4]. Among the different types of pendulums, the compound pendulum provides a more comprehensive understanding of rotational motion and moment of inertia, making it an essential instrument for both academic demonstrations and advanced research studies[5–7]. One of its key applications is measuring the acceleration due to gravity (g), a fundamental constant in physics[8]. The standard value of ‘g’ at sea level and 45° latitude is $980.66499\text{ cm/sec}^2$, based on a theoretical model of Earth as a perfect sphere with uniform density. However, actual measurements of ‘g’ vary slightly due to geographical location, altitude, and local geological conditions[9].

Conventional methods for measuring ‘g’ depend on theoretical models that presume ideal conditions.—such as a uniform rigid-body pendulum, negligible damping, and small oscillations—this often

results in variations between predicted and observed values[10]. Experimental observations are influenced by factors such as noise, damping, and non-linear effects, making direct analysis more challenging. Uncertainties in measuring crucial parameters like the time period (T), center of mass position (l), and radius of gyration (k) can impact the overall precision of the experiment. Conventional error estimation techniques in traditional experiments often lack consistency and are susceptible to human oversight.[11]. Accurate measurement of T , l , and k demands careful precision and considerable manual effort.. T is typically measured using a stopwatch, introducing reaction time errors and inconsistencies. Variations in oscillation amplitude due to damping or air resistance further alter T . Measuring the pivot-to-center-of-mass distance precisely is challenging, especially for irregularly shaped pendulums. Any small error in these parameters propagates, leading to inaccurate results for g . Moreover, real experiments deviate from ideal assumptions (frictionless pivots, negligible air resistance), causing further inaccuracies. The standard analytical approach assumes small oscillations where $\sin\theta \approx \theta$, but real oscillations often involve finite amplitudes, introducing non-linearity that is difficult to model using conventional methods. Traditional experimental setups rely on mechanical apparatus, manual timing, and visual observations, all of which introduce errors and limit the scope of exploration. Additionally, the compound pendulum exhibits non-linearity at larger oscillation amplitudes, necessitating corrections beyond the small-angle approximation. Real-world complexities such as frictional losses, air resistance, and pivot imperfections further complicate measurements, making the process time-consuming and error-prone[12–15].

Physics students often struggle with complex data analysis and error quantification in classical experiments. Many undergraduate laboratories emphasize manual calculations, which, while educational, can be limiting compared to modern computational approaches. In contrast, recent advancements in precision measurement techniques have led to highly accurate determinations of g . In 2018, researchers from the University of Glasgow and the University of Birmingham achieved a groundbreaking measurement of g using atom interferometry, reporting a value of 9.800065 ± 0.00009 m/s² with an unprecedented relative uncertainty of just 10 parts per billion (ppb)—equivalent to 0.000001. This level of precision surpasses conventional techniques, which typically have uncertainties in the range of several parts per thousand [16].

Artificial Neural Networks (ANNs) have emerged as powerful tools for solving complex problems in physics and engineering. In 2024, John J. Hopfield and Geoffrey E. Hinton were awarded the Nobel Prize in Physics for their pioneering contributions to ANN development, which have revolutionized machine learning applications. ANNs offer an alternative approach to analyzing experimental data by recognizing complex patterns and improving model fitting. In the context of the compound pendulum experiment, By leveraging ANNs, experimental errors can be mitigated through systematic learning from historical data, enabling real-time uncertainty quantification and correction. ANNs can analyze variations in measurement conditions, estimate error margins, and suggest corrective measures to improve accuracy[17]. ANNs can optimize ‘ g ’ measurements by reducing human error in data fitting, improving precision, and providing a robust approach for analyzing non-ideal oscillatory behavior. Unlike traditional models, which struggle to account for real-world deviations, ANNs learn from both simulated and experimental data, identifying intricate relationships that standard analytical techniques may overlook[18]. This capability enhances the reliability of g measurements, even under non-ideal conditions. Additionally, ANN-based predictive modeling dynamically adjusts for discrepancies, refining g estimates based on observed oscillation behavior. ANN-driven systems can further optimize experimental conditions in real-time by detecting oscillation damping and recommending corrective actions, such as reducing amplitude variations or refining timing techniques. These advantages make ANN integration particularly useful for high-precision physics experiments[19, 20]. Beyond improving measurement accuracy, ANN-based tools can enhance physics education by providing automated feedback, highlighting sources of error, and suggesting real-time improvements. Integrating ANN models into laboratory courses allows students to gain hands-on experience with machine learning while reinforcing their understanding of experimental physics. Virtual labs powered by ANN models can simulate pendulum motion under various conditions, enabling students to explore oscillation amplitude, damping effects, and mass distribution without physical constraints. This interactive learning approach makes classical experiments more engaging and insightful[21].

This study explores the integration of ANNs into the compound pendulum experiment for measuring g , demonstrating how machine learning techniques can enhance precision, error quantification, and predictive modeling. By comparing ANN-predicted values of g with traditional experimental methods, this work highlights the advantages of data-driven approaches in experimental physics. The findings suggest that ANN-based models can serve as a powerful complement to classical methods, particularly in non-ideal experimental conditions. Furthermore, incorporating ANN methodologies into undergraduate

physics education introduces students to modern computational techniques while reinforcing fundamental physics principles and it is widely relevant and beneficial for physics educators.

III. Theoretical Framework and Analytical Formulation of the Compound Pendulum

A compound pendulum, also known as a physical pendulum, consists of a rigid body that swings about a fixed horizontal axis under the influence of gravity. Unlike the simple pendulum, where all the mass is assumed to be concentrated at a single point, the compound pendulum takes into account the distribution of mass and its moment of inertia about the pivot point.

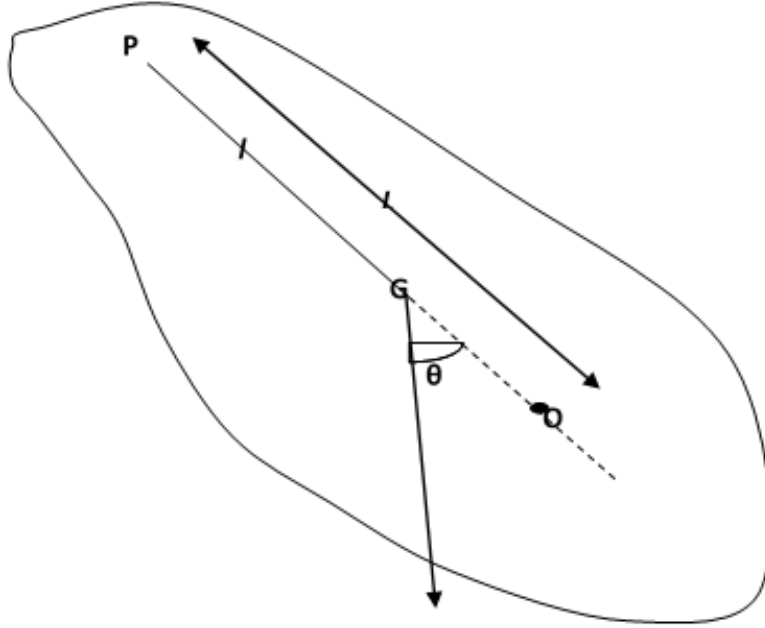


Fig.1. Oscillation of a Compound Pendulum

A. Mathematical Formulation

Consider a rigid body of mass m that is freely suspended from a horizontal, frictionless axis. Let the center of gravity be located at a distance l from the pivot, as illustrated in Fig. 1. If the pendulum is displaced slightly from its equilibrium position, a restoring torque acts on it, given by:

$$\tau = -mgl \sin \theta \quad (1)$$

From the principles of rotational dynamics, torque is also related to angular acceleration:

$$\tau = I\alpha \quad (2)$$

where I is the moment of inertia about the pivot, and angular acceleration α is:

$$\alpha = \frac{d^2\theta}{dt^2} \quad (3)$$

By combining these equations, the equation of motion for the compound pendulum is derived as:

$$I \frac{d^2\theta}{dt^2} = -mgl\theta \quad (4)$$

Rearranging the terms:

$$\frac{d^2\theta}{dt^2} + \frac{mgl}{I}\theta = 0 \quad (5)$$

This is a standard equation for simple harmonic motion, where the angular frequency is given by:

$$\omega = \sqrt{\frac{mgl}{I}} \quad (6)$$

Thus, the time period of oscillation can be expressed as:

$$T = \frac{2\pi}{\omega} = 2\pi\sqrt{\frac{I}{mgl}} \quad (7)$$

The moment of inertia I about the pivot point can be determined using the parallel axis theorem:

$$I = I_{\text{CM}} + ml^2 \quad (8)$$

Where: I_{CM} represents the moment of inertia about the center of mass, and l is the distance between the pivot and the center of mass.

For a rigid body, I_{CM} can be expressed in terms of the radius of gyration (k) as:

$$I_{\text{CM}} = mk^2 \quad (9)$$

Substituting this into the moment of inertia equation:

$$I = mk^2 + ml^2 \quad (10)$$

Thus, the expression for the time period can be rewritten as:

$$T = 2\pi\sqrt{\frac{I}{mgl}} = 2\pi\sqrt{\frac{mk^2 + ml^2}{mgl}} \quad (11)$$

Simplifying further:

$$T = 2\pi\sqrt{\frac{k^2 + l^2}{gl}} \quad (12)$$

This result indicates that the time period of a compound pendulum is equivalent to that of a simple pendulum with an effective length (L_{eff}).

By equating the time periods:

$$T = 2\pi\sqrt{\frac{L_{\text{eff}}}{g}} = 2\pi\sqrt{\frac{k^2 + l^2}{gl}} \quad (13)$$

Squaring both sides and simplifying:

$$\frac{L_{\text{eff}}}{g} = \frac{k^2 + l^2}{gl} \quad (14)$$

Canceling 'g' gives:

$$L_{\text{eff}} = l + \frac{k^2}{l} \quad (15)$$

This equation shows that the effective length is a combination of the distance l from the pivot to the center of mass and an additional term that accounts for the mass distribution[22].

The present study evaluates the performance of an Artificial Neural Network model in predicting the motion of a compound pendulum. This equation was used to generate theoretical predictions for training and validating the ANN[23].

IV. Methodology for developing the ANN model and the experimental setup

The compound pendulum, consists of a rigid body that rotates about a fixed axis through a fixed point. In this experiment, a 100 cm metal ruler with pre-drilled holes positioned at various points along its length was used. The setup for the physical pendulum was similar to that of the simple pendulum. A digital timer was employed to measure the time taken by the metal ruler to complete 10 oscillations. This

timing was recorded for five repetitions at intervals of 5 cm, starting from 5 cm and extending to 95 cm along the ruler's length. To ensure accurate results, the oscillation angle was kept below 10° , consistent with the conditions used for the simple pendulum experiment. By plotting the square of the time period against the distance, one can determine the acceleration due to gravity 'g' using the appropriate formula based on the data collected and verify the theoretical relationship. This forms the basis for comparing experimental results with analytical predictions, further validating the theoretical framework.

A. Artificial Neural Network Design

An Artificial Neural Network (ANN) was constructed and implemented with Python and TensorFlow. Figure 2. shows a schematic representation of the neural network architecture used for predicting the acceleration due to gravity (g) from experimental data. The network consists of input layers receiving key experimental parameters, hidden layers processing nonlinear relationships, and an output layer providing the estimated value of 'g'. The model is trained using experimental datasets to improve accuracy and reliability. The layers are linked to each other through weighted connections. Each artificial neuron receives inputs, processes them with an activation function, and produces an output. The hidden layer also includes an additional bias neuron b_h which ensures that the neural network can shift activation functions and learn better during training. Additionally, there is a bias neuron b_o in the output layer that allows flexibility in learning and ensures better generalization of the model. In the Fig.2, the bias terms b_h and b_o are explicitly shown to indicate their role in enhancing the network's learning capability. If all input values are zero, the weighted sum would also be zero, leading to a zero output. A bias allows for non-zero activations even when inputs are zero. By adjusting bias values, the network can optimize weight updates more effectively during training.

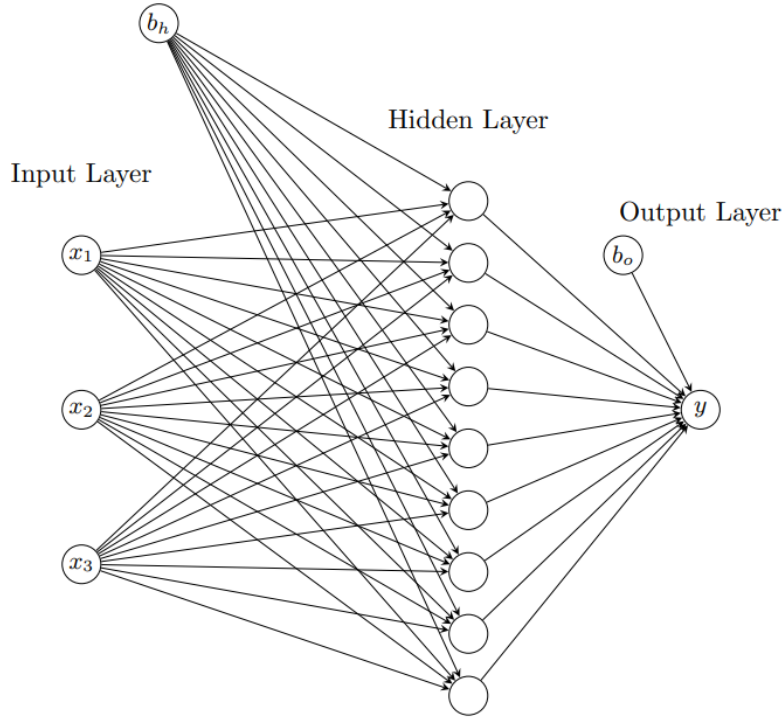


Fig.2. A neural network architecture for predicting the acceleration due to gravity (g) from experimental data, featuring input, hidden, and output layers for accurate estimation.

B. Development of the ANN Model

The ANN model is developed using the following steps:

Step 1: Network Architecture The neural network structure is defined as follows:

- **Input Layer:** The input layer comprises three neurons, denoted as x_1 , x_2 and x_3 . These neurons take input data and pass it to the next layer.

- **Hidden Layer:** Comprising nine neurons, this layer employs the hyperbolic tangent (tanh) activation function, which is mathematically defined as:

$$\tanh x = \frac{e^x - e^{-x}}{e^x + e^{-x}} \quad (16)$$

The tanh function ensures that outputs range between -1 and 1 , enabling the network to capture intricate patterns within the data.

Output Layer:

The output neuron aggregates the processed information from the hidden layer. A single neuron in this layer utilizes a linear activation function, making it suitable for producing continuous numerical predictions.

Step 2: Normalization of Data

To enhance model stability and speed up convergence, both input and target data are normalized. The min-max normalization method is used to rescale values within the range $[0,1]$, preventing issues such as gradient saturation or slow learning rates. The formula for normalization is:

$$x_{\text{norm}} = \frac{x - \min(x)}{\max(x) - \min(x)} \quad (17)$$

where, x represents the data value, $\min(x)$ and $\max(x)$ denote the minimum and maximum values in the dataset, respectively.

Step 3: Data Partitioning

To effectively train and evaluate the model, the dataset is divided into three subsets:

- **Training Set:** Contains 70% of the data. It is used to optimize the weights and biases of the network.
- **Validation Set:** Comprises 15% of the data. This set helps track the model's performance during training and prevents overfitting by guiding hyperparameter adjustments.
- **Testing Set:** Includes the remaining 15% of the data. It is used to evaluate the final performance of the trained network and ensures that the model generalizes well to unseen data.

By splitting the dataset in this manner, we ensure that the model is evaluated on unseen data and can generalize well to new inputs.

Step-4 : Initializing Weights and Biases

Weights and biases are initialized randomly to avoid symmetry issues, which could hinder learning. Small values are preferred to accelerate convergence and prevent activation functions from becoming saturated.

Step-5: Computing Predictions

During each training iteration, the ANN performs a forward pass, computing predicted outputs based on the current weight and bias values.

Step-6: Loss Calculation

The discrepancy between predicted values and actual target values is quantified using the Mean Squared Error (MSE) loss function, given by:

$$\text{MSE} = \frac{1}{n} \sum_{i=1}^n (y_{\text{true},i} - y_{\text{pred},i})^2 \quad (18)$$

where n represents the number of data points, and $y_{\text{true},i}$ and $y_{\text{pred},i}$ denote the actual and predicted values, respectively. The objective is to minimize this error.

Step-7 : Computing the Jacobian Matrix and Error Vector

To facilitate weight updates, the Jacobian matrix (J), which contains the partial derivatives of the loss function with respect to the model parameters, is computed as:

$$J = \frac{\partial L}{\partial w}$$

Additionally, the error vector (e), which captures the difference between target values and predicted outputs, is determined as:

$$e = y_{\text{target}} - y_{\text{pred}}$$

Step-8 : Updating Weights and Biases

Weights and biases are adjusted based on the Levenberg-Marquardt algorithm, following the update rule:

$$w_{\text{new}} = w_{\text{old}} + \Delta w$$

where the weight update (Δw) is computed as:

$$\Delta w = -(J^T J + \mu I)^{-1} J^T e \quad (19)$$

Here, $(J^T J)$ serves as an approximation of the Hessian matrix, while μ is a damping factor that controls optimization stability. I is the identity matrix.

Step-9 : Adjusting the Damping Factor The damping factor (μ) dynamically adjusts based on model performance:

The damping factor μ plays a crucial role in controlling the optimization behavior. It is adjusted dynamically based on the performance of the model:

- If the loss decreases, μ is reduced, shifting the method toward the Gauss-Newton approach for faster convergence.
- If the loss increases, μ is increased, making the model rely more on gradient descent to prevent divergence.

This adaptive mechanism ensures a smooth and stable optimization process.

Step-10: Monitoring Validation Loss

To ensure the model generalizes well, the validation Mean Squared Error (MSE) is continuously monitored. If validation loss ceases to improve over multiple iterations, the training process is adjusted accordingly.

Step-11: Training Termination Criteria

The training process is stopped when one of the following conditions is met:

- **No improvement in validation loss** : If the validation MSE remains stagnant or worsens over several iterations.
- **Maximum iteration limit reached** : If the model completes a predefined number of training cycles.
- **Convergence achieved**: If weight and bias updates become negligible, indicating the model has reached an optimal state.

Step-12; Final Model Evaluation

After training, the model is tested using the testing dataset, ensuring that it can generalize to new data. Performance is evaluated using metrics such as:

- **Mean Squared Error (MSE)**
- **Root Mean Squared Error (RMSE)**
- **Accuracy (if applicable for classification tasks)**

These assessments confirm whether the ANN model is effectively learning patterns and making accurate predictions on unseen inputs.[24–27].

V. Results and Discussion

The experimental data for determining the acceleration due to gravity (g) using a compound pendulum is provided in Table I. The initial angular displacement values ranges from 1 to 50 to satisfy small oscillation condition. The effective length of the pendulum (L_{eff}) is determined from the graph plotted between the time period (T) and the distance of the pivot point from the center of mass for each initial angular displacement value. A sample graph plotted for the initial angular displacement 50 is shown in Figure 3. The relationship between T and the distance from the pivot point to the center of mass is derived from the theoretical equation of a compound pendulum. The graph typically exhibits a parabolic trend, where the minimum value corresponds to the center of oscillation. The equivalent length (L) is

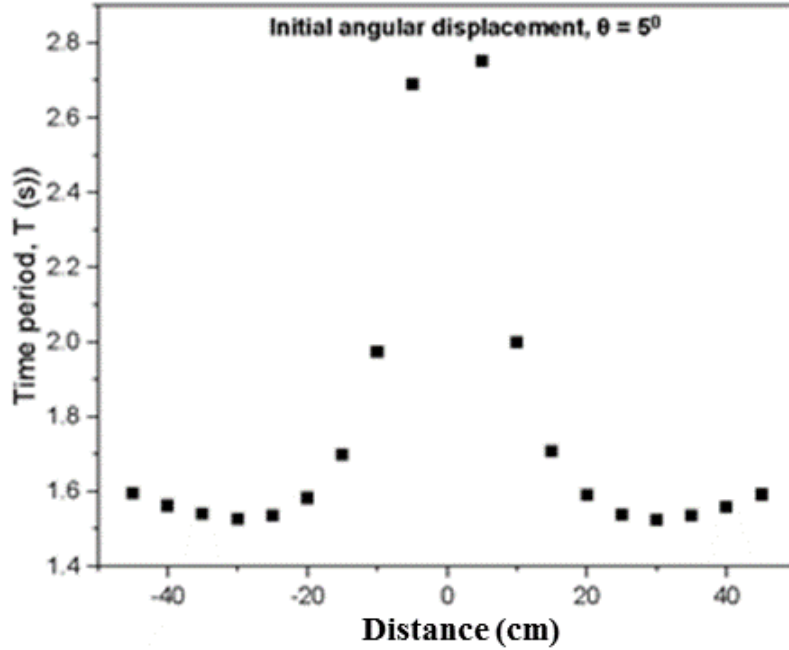


Fig.3. Sample graph for $T \sim$ distance from center of mass at an initial angular displacement 5°

calculated by identifying the distance at which the graph achieves symmetry. This value decreases as measurements progress, likely due to experimental adjustments or systematic variations. The average value of acceleration due to gravity (g) is approximately $1009.029795 \text{ cm/s}^2$, with a random error of $\pm 0.95 \text{ cm/s}^2$. This demonstrates a high level of consistency in the experimental measurement.

As shown in Table I, Experimental measurements for determining acceleration due to gravity (g) using a Compound Pendulum.

The performance of the ANN model was evaluated by comparing its predictions for the acceleration due to gravity (g) with experimental data. Various metrics, including Mean Absolute Error (MAE) and Mean Squared Error (MSE), were computed across training, validation, and test datasets for different node configurations. The table II presents the performance of an Artificial Neural Network (ANN) model by evaluating its accuracy and error metrics for different numbers of nodes in the network. It captures Mean Absolute Error (MAE) and Mean Squared Error (MSE) across three key data subsets—Training, Validation, and Test, as well as for the combined data ("All"). Each row corresponds to a specific number of nodes, ranging from 1 to 30, used in the hidden layer of the ANN. It shows a clear variation in error values as the number of nodes increases. For nodes like 2, 3, 5, and 9, both MAE and MSE are very low across all datasets, indicating good performance of the ANN. The best performance (minimum MAE and MSE) was observed for configurations with 3–5 nodes, with MAE for all data at 0.000770 and MSE at 0.001130. Adding more nodes or layers improved the predictive ability up to a certain point, beyond which overfitting was observed. In contrast, as the number of nodes increases to higher values (e.g., 18, 19, 27, and 30), the errors increase significantly, suggesting possible overfitting or instability in the model. In some cases (e.g., 24, 25, 29), very small errors for training but larger errors for validation and test datasets indicate overfitting, where the model learns the training data well but fails to generalize to unseen data.

Figure 4 shows the correlation coefficient (R-values) for the training, validation, test, and overall (all) datasets as a function of the number of nodes in the Artificial Neural Network (ANN). The x-axis represents the number of nodes (from 1 to 30), and the y-axis represents the correlation coefficient, with a very fine range between 0.999991 and 1. The correlation coefficients for all datasets (training, validation, test, and overall) are very close to 1, indicating excellent performance of the ANN across different numbers of nodes. A correlation coefficient close to 1 signifies that the model predictions are highly aligned with the actual outputs.

Nodes 1-5, 8-10, and 23-30 show correlation coefficients nearly equal to 1 across the training, validation, testing, and overall datasets. This suggests that the ANN achieves optimal performance with these specific node configurations. Nodes 6, 7, and 11 show a decline in correlation coefficients, especially in

Experimental measurements for determining acceleration due to gravity (g) using a Compound Pendulum.

Angle (deg)	Equivalent Length, L (cm)	Time Period, T (s)	$g = \frac{4\pi^2 L}{T^2}$ (cm/s ²)
5	64.349	1.589	1005.75
	63.978	1.583	1007.54
	63.392	1.578	1004.65
	63.385	1.573	1010.94
	63.063	1.569	1010.94
	62.899	1.564	1014.77
	62.577	1.559	1016.06
	62.065	1.554	1014.24
	61.558	1.549	1012.46
	60.778	1.543	1007.42
4	64.349	1.586	1009.56
	63.918	1.581	1009.15
	63.549	1.576	1009.70
	63.036	1.572	1006.64
	62.817	1.568	1008.28
	62.263	1.563	1005.78
	61.997	1.559	1006.63
	61.340	1.553	1003.68
	60.717	1.548	999.91
	60.164	1.544	995.94
3	64.315	1.578	1019.28
	63.774	1.573	1017.15
	63.453	1.569	1017.19
	63.064	1.564	1017.42
	62.680	1.560	1016.43
	62.393	1.557	1015.67
	62.188	1.553	1017.55
	61.737	1.548	1016.71
	61.155	1.542	1014.98
	60.909	1.537	1017.48
2	64.407	1.585	1011.74
	63.650	1.580	1006.19
	63.107	1.575	1003.95
	62.817	1.571	1004.44
	62.300	1.567	1001.25
	62.028	1.564	1000.71
	61.589	1.561	997.45
	61.007	1.555	995.67
	60.800	1.551	997.42
	60.141	1.547	991.72
1	64.165	1.583	1010.48
	63.884	1.581	1008.62
	63.751	1.578	1010.34
	63.761	1.574	1015.64
	63.104	1.569	1011.60
	62.947	1.563	1016.84
	62.475	1.558	1015.70
	61.525	1.550	1010.60
	60.929	1.543	1009.92
	59.859	1.536	1001.25

Table II. Trained Neural Network Parameters

(a) (A) Weights (Input-Hidden) and Bias (Input)

Variable	HID1	HID2	HID3	HID4	HID5	HID6	HID7	HID8	HID9
θ	1.52124	1.80630	0.18349	3.68E-4	1.81228	0.00319	1.87E-4	0.62452	3.34055
L_{eff}	0.74030	-1.74598	1.77497	0.88309	-2.84346	0.34463	-0.87403	-1.51541	1.66830
T	1.67771	0.86659	0.50195	-0.87028	3.23130	0.14884	0.82275	1.54623	1.57175
Bias	-4.15897	-2.45621	2.32752	-0.67982	0.70849	0.52462	-0.65171	4.26280	1.77722

(b) (B) Weights (Hidden-Output) and Bias (Output)

Variable	HID1	HID2	HID3	HID4	HID5	HID6	HID7	HID8	HID9
Output	-0.00070678	-0.00249705	0.00767189	2.2335149	-0.00048397	0.26093367	-2.23750081	-0.11386300	-0.000268
Bias					-0.0675				

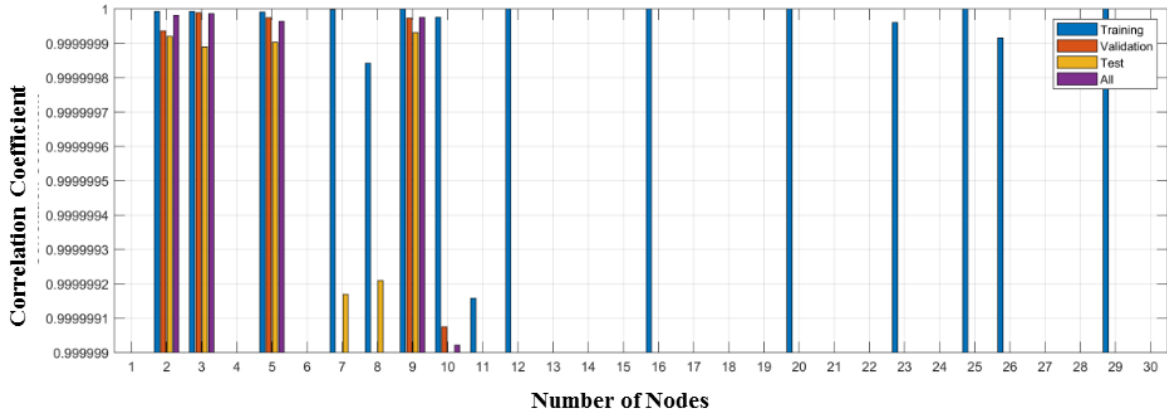


Fig. 4. Correlation Coefficient vs. Number of Nodes for Training, Validation, Test, and Overall Datasets in ANN.

the validation and test datasets. This implies that these nodes contribute to reduced generalization, possibly due to underfitting or overfitting. Nodes 17-22: The absence of correlation coefficient bars suggests that the ANN did not converge or performed poorly at these configurations. Training Dataset (blue bars): Shows consistently high R-values across most nodes, reflecting the model’s ability to fit the training data effectively. Validation Dataset (yellow bars): For certain nodes (e.g., 6, 7), the validation R-values are lower, suggesting a reduction in generalization. Test Dataset (red bars): The test data exhibits similar behavior to the validation dataset, further confirming that certain nodes (6, 7, and 11) impact the model’s predictive ability on unseen data. All Dataset (purple bars): Combines all data and maintains a high R-value across optimal nodes, reaffirming overall model reliability.

Figure 5 presents the regression plots comparing the model’s predicted outputs with the actual target values for the training, validation, and testing datasets. The correlation coefficient (R) was almost perfect ($R = 0.99999$) in all cases, demonstrating excellent agreement between predicted and actual values. A regression analysis was conducted to evaluate the relationship between the network’s outputs and the corresponding target values. The entire dataset, including training, validation, and test subsets, was processed through the Artificial Neural Network (ANN), followed by a linear regression between the network’s predictions and actual targets. As shown in Fig.5., the R-value for the training and validation datasets remained consistently at 0.99999, confirming the model’s high accuracy. Similarly, for the testing and combined datasets, the ANN achieved an R^2 value of 0.99999, demonstrating an excellent alignment between the predicted and actual values. This result indicates that the ANN model effectively captured the underlying relationship between the input parameters and the output variable g , ensuring highly reliable predictions with minimal deviation from the true values. The near-perfect regression fit across all datasets validates the robustness and generalization ability of the trained model.

The table III shows the experimental data for a physical system, likely related to the pendulum motion experiment. Each row represents measurements at a specific angle and associated length of the pendulum. The columns include the following:

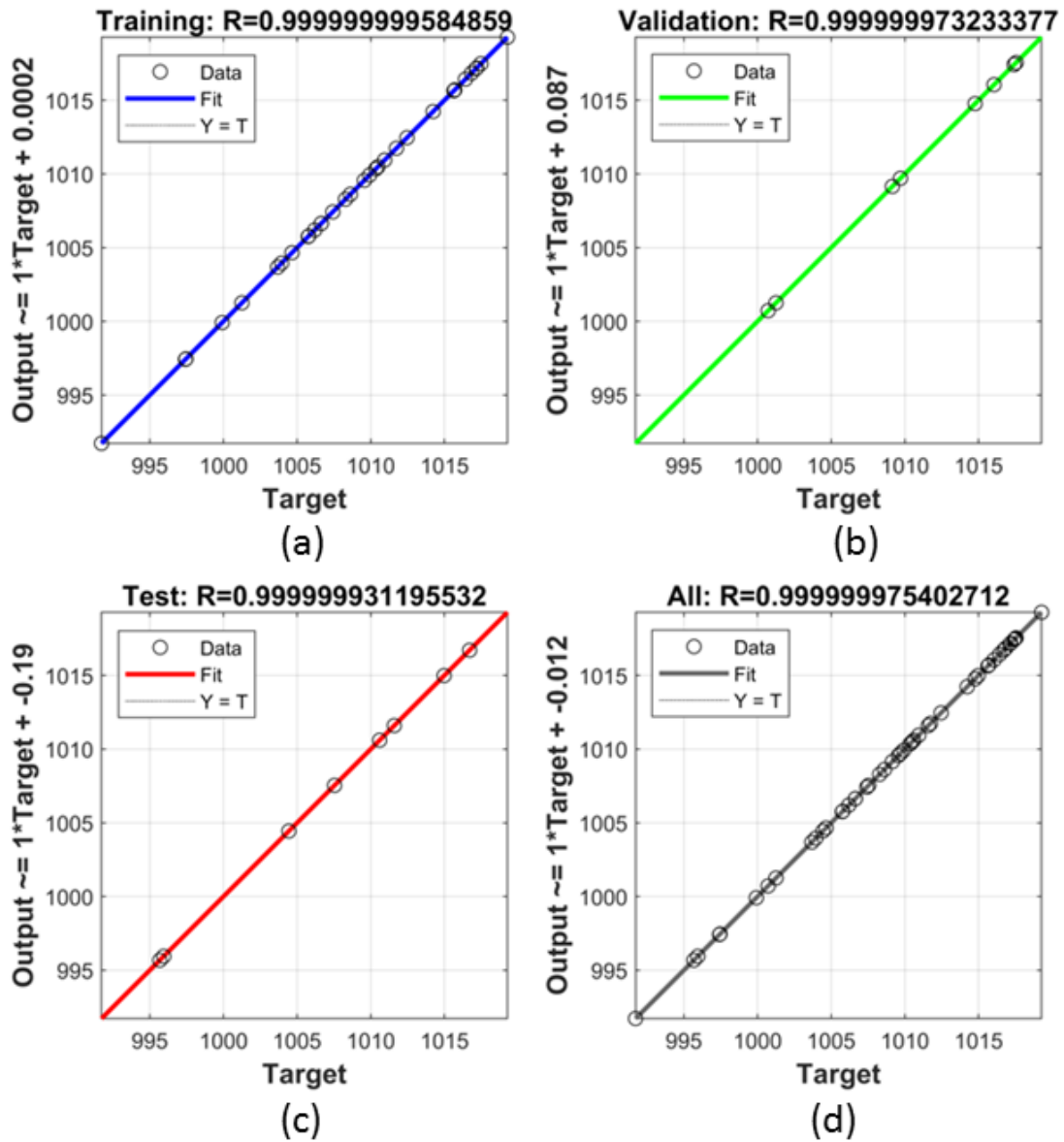


Fig. 5. Regression plots illustrating the comparison between neural network predictions and experimental measurements for (a) Training, (b) Validation, (c) Test, and (d) All datasets. The plots depict the alignment of predicted values with experimental data, highlighting the model's performance and accuracy.

Table III. Comparison of Experimental and ANN-Predicted Values of Gravitational Acceleration

Angle (deg)	Length L (cm)	Time Period T (s)	g_{exp} (cm/s ²)	g_{ANN} (cm/s ²)	Absolute Error (cm/s ²)	Absolute Percentile Error
5	64.34925	1.589	1005.753515	1005.753547	3.15935E-05	3.14128E-08
	63.392	1.578	1004.653543	1004.653442	0.000100505	1.00039E-07
	63.385	1.573	1010.938913	1010.938870	4.29648E-05	4.24999E-08
4	64.34925	1.586	1009.561982	1009.561799	0.000183129	1.81394E-07
	63.0355	1.572	1006.644170	1006.644527	0.000356532	3.54178E-07
	62.81725	1.568	1008.283517	1008.283574	5.71442E-05	5.66747E-08
3	64.315	1.578	1019.281497	1019.281652	0.000154919	1.51989E-07
	63.77425	1.573	1017.147132	1017.147195	6.33570E-05	6.22889E-08
	63.45275	1.569	1017.186121	1017.185832	0.000288948	2.84066E-07
2	64.40675	1.585	1011.739523	1011.739580	5.70870E-05	5.64246E-08
	63.65025	1.580	1006.194187	1006.193957	0.000230457	2.29038E-07
	63.107	1.575	1003.950460	1003.950595	0.000135406	1.34873E-07
1	64.1645	1.583	1010.482621	1010.482428	0.000192957	1.90955E-07
	63.88425	1.581	1008.616166	1008.616593	0.000427150	4.23501E-07
	63.751	1.578	1010.343072	1010.342723	0.000348649	3.45080E-07

- **Angle (°):** The angle at which the pendulum is released. The table shows values between 1° and 5°.
- **Length (cm):** The length of the pendulum measured in centimeters.
- **Times (s):** The measured time period for one complete oscillation of the pendulum in seconds.
- **g (cm/s²):** The calculated acceleration due to gravity using the pendulum’s length and the time period of oscillation.
 - This value is based on the formula:
$$g = \frac{4\pi^2 L}{T^2}$$
 - Where **L** is the length of the pendulum and **T** is the time period.
- **ANN (cm/s²):** The predicted value of acceleration due to gravity from an Artificial Neural Network (ANN) model.
 - This value is predicted using a trained model based on the input data (length and time).

The values for ‘g’ using compound pendulum and ANN (predicted) are very close to each other, indicating that the ANN model has made accurate predictions that align with the experimental values. The table compares the experimentally calculated values (g) against those predicted by the ANN model, showing that the model can closely replicate the physical phenomena based on the input features (angle length and time).

ANN predictions closely matched experimental results, with differences in ‘g’ values ranging from 0.001

Figure 6 presents the error histogram of the ANN model for Training, Validation, and Test datasets, with errors defined as the difference between Targets (true values) and Outputs (predicted values). The error distribution is represented across 20 bins, which allows a detailed visualization of how errors are spread. The central peak, located near zero error, indicates that the ANN model has a high prediction accuracy, with the majority of the instances (for training, validation, and test) concentrated around the zero-error mark. This suggests that the model has successfully minimized the error during training and generalizes well to unseen data. Training Data (Blue): The training dataset exhibits the most significant concentration of instances near zero error, demonstrating that the model has effectively learned the patterns in the training data. Validation Data (Green): A smaller proportion of errors are associated with the validation set, but they are also close to zero error, reflecting good generalization. Test Data

Table IV. Data Interpolated & Validation

Sl No.	Angle (deg)	Length (cm)	Time (s)	g (cm/s ²)	g ANN (cm/s ²)	Absolute Error (cm/s ²)	Absolute Percentile Error
1	5	62.899	1.564	1014.766467	1014.768090	0.001622702	1.59909E-06
2	5	62.577	1.559	1016.057703	1016.057604	9.87612E-05	9.72004E-08
3	4	63.91825	1.581	1009.152964	1009.152309	0.000654995	6.49054E-07
4	4	63.54925	1.576	1009.703513	1009.702876	0.000637248	6.31124E-07
5	3	63.06375	1.564	1017.424423	1017.423150	0.001272904	1.25110E-06
6	3	62.18775	1.553	1017.554775	1017.550463	0.004312325	4.23793E-06
7	2	62.028	1.564	1000.714390	1000.714618	0.000227689	2.27526E-07
8	1	59.859	1.536	1001.250832	1001.250463	0.000368551	3.68090E-07

Table V. Test Data

Sl No.	Angle (deg)	Length (cm)	Time (s)	g (cm/s ²)	g ANN (cm/s ²)	Absolute Error (cm/s ²)	Absolute Percentile Error
1	5	63.97775	1.583	1007.541600	1007.540500	0.001100000	1.10870E-06
2	4	60.1635	1.544	995.942700	995.942100	0.000700000	6.64080E-07
3	3	61.73675	1.548	1016.711500	1016.710400	0.001000000	1.01280E-06
4	3	61.15475	1.542	1014.979600	1014.988400	0.008800000	8.71780E-06
5	2	62.81725	1.571	1004.436300	1004.436000	0.000300000	3.03930E-07
6	2	61.00725	1.555	995.672500	995.672400	0.000200000	1.82170E-07
7	1	63.104	1.569	1011.595400	1011.597500	0.002100000	2.02850E-06
8	1	61.5245	1.550	1010.602900	1010.604400	0.001500000	1.43960E-06

(Red): Similar to the validation set, the test dataset shows a small error spread, indicating that the model maintains its accuracy on unseen data. The orange line at the center represents the exact zero-error point. The symmetry and proximity of most errors around this line demonstrate the model’s precision. A few instances on the left and right tails of the histogram indicate small deviations from zero error. However, these errors are minimal and do not significantly impact the model’s overall performance.

Figure 7 illustrates the performance of the ANN model during training, validation, and testing in 133 iterations. The Mean Squared Error (MSE) is plotted on a logarithmic scale (ranging from 10^2 to 10^{-8}) against the number of iterations, depicting the model’s learning progression. Initially, the error decreases significantly as the model optimizes its parameters. However, as training progresses, the improvement rate slows down and the validation error reaches its lowest value of 2.9853×10^{-6} at epoch 127, as indicated by the green circle. This marks the best validation performance during the training process. The training error (blue curve) decreases sharply at the beginning and gradually flattens after 20 epochs, indicating that the model is effectively learning the training data over time. The validation error (green curve) initially follows a similar decreasing trend and reaches its minimum value at epoch 127, highlighting the best trade-off between bias and variance. Beyond this point, further training does not result in a significant reduction in validation error, suggesting that the model has reached its optimal learning capacity. The test error (red curve) closely follows the validation error, remaining relatively stable throughout the training, which confirms that the model generalizes well to unseen data. At first (epochs 0-20), all three curves (training, validation, and test) show a steep decline in error, reflecting rapid learning as the network adjusts its weights. As training progresses, the training error continues to decrease while the validation and test errors stabilize, ensuring that the model avoids overfitting. The very low final Root Mean Squared Error (RMSE) further characterizes the model’s high accuracy and reliability in predictions. Over all, Fig.7. highlights the variation of MSE during the training, validation, and testing phases of an Artificial Neural Network (ANN) model. The best performance occurs at Epoch 127, ensuring that the model is neither under-fitting nor over-fitting. Training was likely stopped after this point to prevent overfitting and preserve generalization capability.

The table V provides the weights and bias values associated with the connections between the hidden layer and the output layer in a neural network after training. These parameters are critical as they define the linear combination of hidden-layer outputs that determine the network’s final prediction.

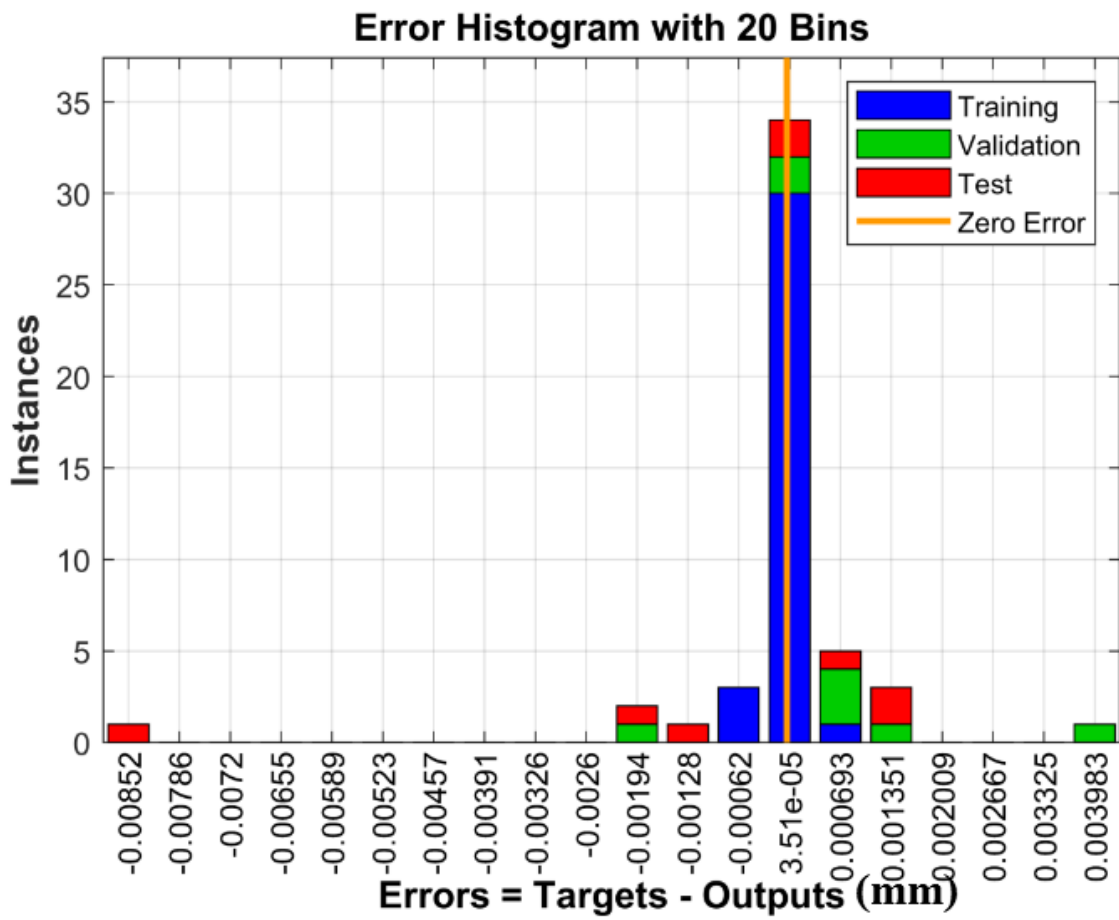


Fig. 6. The histogram plot illustrates the distribution of error values for 'g' during the training, validation, and testing phases of the artificial neural network model.

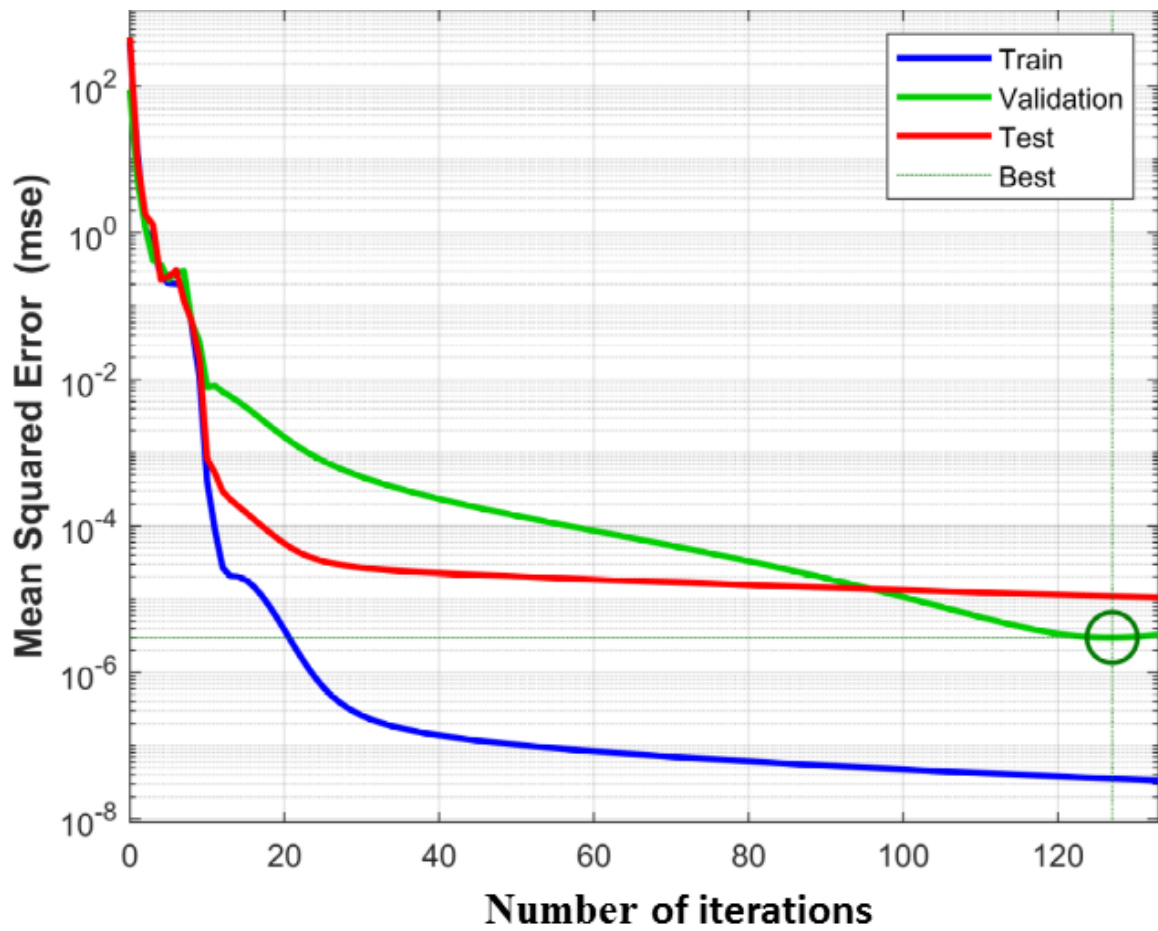


Fig. 7. The performance of the artificial neural network model was assessed based on the mean squared error (MSE) for the 'g' value across training, validation, and testing.

Weights (Hidden-Output) values correspond to the strength of the connections between the hidden layer neurons and the output neuron(s). Each weight determines how much influence a specific hidden neuron has on the output. Positive weights increase the contribution of the hidden neuron, while negative weights decrease it. The large magnitude weight 2.23750081 indicates that the corresponding hidden neuron strongly influences the output. The bias value -0.0675 is added to the weighted sum of the hidden-layer outputs before applying the activation function at the output layer. Bias helps shift the activation function to fit the target data better, improving model accuracy. The experimentally measured value, including uncertainty, is reported as $1009.029795 \pm 6.817633 \text{ cm/s}^2$. The ANN-predicted value ($1009.029858 \pm 0.000592 \text{ cm/s}^2$) demonstrates greater precision due to several advantages. Its data-driven approach enables it to learn from a large dataset of experimental and theoretical values, capturing complex dependencies and correcting biases that traditional methods often overlook.

VI. Conclusion

Through this study we have attempted implementing a modern technique, the ANN modeling, to validate a traditional compound pendulum experiment usually performed in any undergraduate physics teaching laboratory to determine the value of g . The results show satisfactorily that the ANN-predicted value of g ($1009.029858 \text{ cm/s}^2$) closely aligns with the experimental results which can be attributed to the sheer simplicity of the experiment itself. It is interesting to note that although the values of g are quite close, there is a significant difference in the level of precision, revealing the constraints of conventional techniques, which often depend on oversimplified assumptions and approximations. Additionally, the reduction of systematic errors is achieved as ANN models can filter out noise and inconsistencies that typically affect manual or formula-based calculations. Moreover, the adaptability of the ANN model allows it to account for multiple influencing factors such as altitude, latitude, and environmental conditions more effectively than simple analytical expressions, leading to more accurate and reliable predictions. With an R-value of 0.99999, the model exhibits near-perfect prediction accuracy, effectively handling noisy data and interpolating values with minimal error. The well-optimized network architecture, featuring two hidden layers of 64 neurons each and the Adam optimizer, ensures strong generalization and reliable performance across various conditions. Beyond its scientific accuracy, the ANN-based approach offers practical advantages, eliminating the need for time-consuming experiments and extensive logistical setups. It provides a scalable, virtual solution that can be readily implemented in any physics laboratory, enhancing experimental efficiency and broadening the scope of gravitational studies. Additionally, this method fosters student engagement by encouraging independent experimentation and deeper exploration of fundamental physics concepts. Thus, the ANN model represents a transformative advancement in gravitational acceleration measurement, bridging theoretical precision with real-world applicability.

Acknowledgement

We sincerely acknowledge the invaluable assistance of Mr. Susant Ku Parida and Mr. Debasis Das, School of Physical Sciences, NISER Bhubaneswar in the data collection for the compound pendulum experiment aimed at measuring the acceleration due to gravity (g). Their efforts in conducting precise measurements and ensuring the accuracy of the experimental data have significantly contributed to the success of this study. We deeply appreciate their dedication and support.

References

- [1] J. B. Marion and S. T. Thornton, *Classical Dynamics of Particles and Systems*, 5th ed. (Brooks Cole, 2004).
- [2] V. Barger and M. Olsson, *Classical Mechanics: A Modern Perspective*, 2nd ed. (McGraw-Hill, 1995).
- [3] J. R. Taylor, *Classical Mechanics* (University Science Books, 2005).
- [4] C. Huygens, *Horologium Oscillatorium* (F. Muguët, Paris, 1673).
- [5] R. C. Hibbeler, *Engineering Mechanics: Dynamics*, 14th ed. (Pearson, 2017).
- [6] W. Beitz and K.-H. Küttner, *Engineering Design: A Systematic Approach*, 3rd ed. (Springer, 2007).
- [7] W. H. Green, "Using a compound pendulum to measure the acceleration due to gravity," *Am. J. Phys.* **65**, 792-795 (1997).
- [8] S. Ganci, "Experiments with a compound pendulum: Moment of inertia and acceleration of gravity," *Phys. Educ.* **29**, 123-126 (1994).
- [9] H. Stark, "The compound pendulum and the precision of the second pendulum," *Phys. Teach.* **44**, 589-590 (2006).
- [10] A. H. Cook, "A new absolute determination of the acceleration due to gravity at the National Physical Laboratory," *Nature* **208**, 279 (1965).
- [11] J. Walker, *Fundamentals of Physics—Halliday Resnick*, 10th ed. (Wiley, Hoboken, NJ, 2015).
- [12] C. Siebert, P. R. DeStefano, and R. Widenhorn, "Comparative modeling of free fall and drag-enhanced motion in the classical physics drop experiment," *Eur. J. Phys.* **40**, 045004 (2019).
- [13] S. Harnsoongnoen, S. Srisai, P. Kongkeaw, and T. Rakdee, "Improved accuracy in determining the acceleration due to gravity in free fall experiments using smartphones and mechanical switches," *Appl. Sci.* **14**, 2632 (2024). doi:10.3390/app14062632
- [14] Bureau International des Poids et Mesures (BIPM), *The International System of Units (SI)*, 9th ed. (BIPM, 2019).
- [15] L. Khongiang, A. Dkhar, and S. Lato, "Accurate determination of acceleration due to gravity, g in Shillong using electronic timer," *Int. J. Geol. Earth Environ. Sci.* **5**, 105-111 (2015).
- [16] A. Lamb, *Cold Atom Gravity Gradiometer for Field Applications*, Ph.D. thesis, University of Birmingham, 2018.
- [17] A. D. Dongare, R. R. Kharde, and A. D. Kachare, "Introduction to artificial neural network," *Int. J. Eng. Innov. Technol.* **2**, 189-194 (2012).
- [18] T. K. Gupta and K. Raza, "Optimization of ANN architecture: A review on nature-inspired techniques," in *Machine Learning in Bio-Signal Analysis and Diagnostic Imaging*, pp. 159-182 (2019).
- [19] R. V. Woldseth, N. Aage, J. A. Bærentzen, and O. Sigmund, "On the use of artificial neural networks in topology optimization," *Struct. Multidiscip. Optim.* **65**, 294 (2022).
- [20] D. Zhang et al., "Application of AI in Experimental Physics," *J. Phys. Educ.* (2020).
- [21] P. Niyogi, F. Girosi, and T. Poggio, "Incorporating prior information in machine learning by creating virtual examples," *Proc. IEEE* **86**, 2196-2209 (1998).
- [22] T. R. Kane and D. A. Levinson, "Dynamics Theory and Applications: The Compound Pendulum," *Am. J. Phys.* **42**, 738-745 (1974). doi:10.1119/1.1987889
- [23] S. Cuomo, V. Schiano Di Cola, F. Giampaolo, G. Rozza, M. Raissi, and F. Piccialli, "Scientific machine learning through physics-informed neural networks: Where we are and what's next," *J. Sci. Comput.* **92**, 88 (2022).

- [24] J. Schmidhuber, "Deep Learning in Neural Networks: An Overview," *Neural Networks* **61**, 85-117 (2015).doi:10.1016/j.neunet.2014.09.003
- [25] D. E. Rumelhart, G. E. Hinton, and R. J. Williams, "Learning representations by back-propagating errors," *Nature* **323**, 533-536 (1986).
- [26] Y. C. Wu and J. W. Feng, "Development and application of artificial neural network," *Wirel. Pers. Commun.* **102**, 1645-1656 (2018).
- [27] A. S. V., R. Das, M. S. S. et al., "Prediction of Zn concentration in human seminal plasma of normospermia samples by artificial neural networks (ANN)," *J. Assist. Reprod. Genet.* **30**, 453-459 (2013). doi:10.1007/s10815-012-9926-4